Underground Mining Technology 2017 – M Hudyma & Y Potvin (eds)

doi:10.36487/ACG_rep/1710_31_Yang

Numerical and limit equilibrium stability analyses of cemented mine backfill upon vertical exposure

PY Yang *Polytechnique Montreal, Canada*

L Li *Polytechnique Montreal, Canada*

Abstract

In open stope mines, the cemented backfill must maintain self-standing in the primary stope during the extraction of an adjacent secondary stope. A limit equilibrium solution proposed by Mitchell et al. (1982) has been widely used since the 1980s to design the exposed cemented fill. This solution has been the object of several modifications over the years. Recently, the comparison between these solutions and numerical simulations indicated that the former are not fully representative of the exposed fill when its required cohesion is relatively large. In this paper, new numerical results show that the slip surface transitions from planar at low fill cohesion to spoon-shaped at larger cohesion. In the former case, the failure is controlled by shear stresses mobilised along the planar slip surface. This is very similar to the failure mode assumed in existing theoretical models. In the latter case, however, the failure is governed by both shear (near the base) and tensile (near the top) stresses, indicating a different failure mode. Based on these observations, a new analytical solution is proposed to evaluate the stability of side-exposed cemented fill. This solution is validated using complementary simulations and the results indicate that the two different approaches agree well for typical stope geometry and fill properties.

Keywords: *exposed mine backfill, Mitchell et al. solution, limit equilibrium, numerical modelling*

1 Introduction

In open stoping, stopes are usually divided into primary and secondary stopes to facilitate pillar recovery (Mitchell et al. 1982; Pierce 2001; Emad et al. 2014). The primary stope is first mined and then backfilled with cemented fill, which acts as an artificial rib pillar during extracting a secondary stope.

Before the 1980s, the exposed cemented fill was designed as a freestanding vertical prism (1D) or a 2D vertical slope (e.g. Askew et al. 1978). These methods ignore the confinement exerted by the remaining stope walls, leading to over-conservative design. Mitchell et al. (1982) developed the well-known 3D wedge model that has been widely applied with a significant save in binder usage. Several modifications of the Mitchell et al. (1982) solution have been made in past years (Zou & Nadarajah 2006; Dirige et al. 2009; Li & Aubertin 2012, 2014; Li 2014).

Recently, Falaknaz and co-workers (Falaknaz 2014; Falaknaz et al. 2015) conducted simulations using FLAC3D to evaluate the stress state in the backfilled stope with an open face. The comparisons between their simulation results and several analytical solutions indicated that the effect of stope size on the required fill strength is not always well-reflected by the latter. A new solution is thus required.

In this study, simulations conducted with FLAC3D are used to assess the stability of exposed fill based on a more objective instability criterion. A new solution is then proposed to estimate the required strength of exposed cemented fill upon vertical exposure, based on a failure mode observed in numerical simulations and experimental tests. The new solution is validated using additional numerical simulations.

2 Existing analytical solutions

2.1 Mitchell et al. (1982) solution

Figure 1 shows the wedge model of a side-exposed cemented fill considered by Mitchell et al. (1982). L (m), B (m) and H (m) represent the length, width and height of the backfill. The inclination angle of the sliding surface α is taken as 45° + ϕ/2 (to the horizontal). It is assumed that the stope has a high aspect ratio (HAR, $H/B \geq \tan\alpha$) so that the sliding plan is limited within the fill body. It is considered that only the cohesion of fill–sidewall interface c_s (assumed equal to the backfill cohesion c) contributes to the shear strength mobilised along the sidewalls. There is no shear strength mobilised along the back wall. The Factor of Safety (FS) and the required backfill cohesion c of the exposed backfill are given by:

$$FS = \frac{\tan\phi}{\tan\alpha} + \frac{2cL}{H^*(\gamma L - 2c_s)\sin 2\alpha} \tag{1a}$$

$$c = \frac{\gamma H}{2(H/L + \tan\alpha)}, \text{ for FS = 1, } c = c_s \text{ and } H >> B \text{ thus } H^* \approx H \tag{1b}$$

where:

H^* [= H – (Btanα)/2, m] is the equivalent height of the sliding wedge.

γ (kN/m^3), ϕ (= ϕ', °) and c (= c', kPa) are the fill's unit weight, internal friction angle and cohesion.

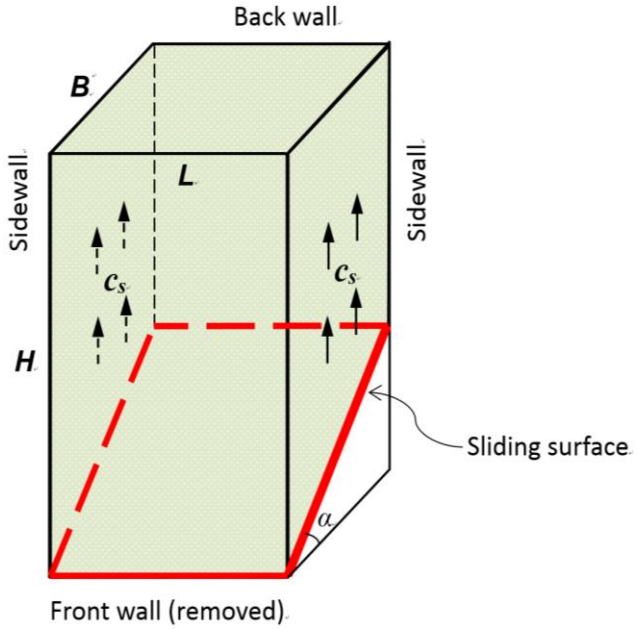

Figure 1 Mitchell et al.'s wedge model (adapted from Mitchell et al. 1982)

This solution has been the objective of several modifications over the years.

2.2 Modifications of the Mitchell solution

Li & Aubertin (2012) extended the Mitchell et al. (1982) solution by considering surcharge p_0 (kPa), different stope aspect ratios, and reduced interface cohesion along sidewalls. For a HAR stope, the sliding surface develops within the backfill. The required fill cohesion c can be expressed as:

$$c = \frac{p_0 + \gamma H^*}{\frac{2}{(FS - \tan\phi'/\tan\alpha)\sin 2\alpha} + \frac{2r_s H^*}{L}} \quad (2)$$

where:

r_s (= c_s/c; from 0 to 1) is the adherence ratio along the sidewalls.

The sliding surface may be extended to the backfill top for low aspect ratio (LAR, $H/B < \tan\alpha$) stopes. This consideration leads to the following expression:

$$c = \frac{p_0 + \gamma H/2}{\frac{2}{(FS - \tan\phi'/\tan\alpha)\sin 2\alpha} + \frac{r_s H}{L}} \quad (3)$$

When there is a tension crack, Li & Aubertin (2012) assumed that its depth H_t (m) can be expressed as (based on the theory of Rankine's active earth pressure; McCarthy (2002)):

$$H_t = \frac{2c}{\gamma \tan(45° - \phi'/2)} \quad (4)$$

The equivalent width of the sliding wedge B_t is then written as:

$$B_t = (H - H_t)/\tan\alpha \quad (5)$$

The stability of an exposed backfill face or the required cohesion can then be assessed by replacing B in Equation 2 with the equivalent wedge width B_t.

Li (2014) modified the Li & Aubertin (2012) solution by considering the frictional strength along the sidewalls and interface cohesion along the back wall c_b. For HAR stopes, the required fill cohesion c is given by:

$$c = p'\left[\frac{2}{(FS - \tan\phi'/\tan\alpha)\sin 2\alpha} + r_b\frac{H - B\tan\alpha}{B} + 2r_s\frac{H^*}{L}\right]^{-1} \quad (6a)$$

with

$$p' = \frac{L}{2K\tan\delta}\left\{\gamma - \frac{1}{B\tan\alpha}\left(\frac{\gamma L}{2K\tan\delta} - p_0\right)\times\left[\exp\left(-\frac{2K\tan\delta}{L}(H - B\tan\alpha)\right) - \exp\left(-\frac{2K\tan\delta}{L}H\right)\right]\right\} \quad (6b)$$

where:

r_b (= c_b/c; from 0 to 1) is the adherence ratio along the back wall.

δ (°) is the friction angle along the sidewalls (varying from zero to ϕ').

K is the earth pressure coefficient along sidewalls; its value is taken as Rankine's coefficient K_a. This is very similar to the case of cohesive soil with a vertical open face (Bowles 1984).

In the case of LAR stopes, the Li (2014) solution is expressed as:

$$c = p''\left[\frac{2}{(FS - \tan\phi'/\tan\alpha)\sin 2\alpha} + r_s\frac{H}{L}\right]^{-1} \quad (7a)$$

with

$$p'' = \frac{L}{2K\tan\delta}\left\{\gamma - \frac{1}{H}\left(\frac{\gamma L}{2K\tan\delta} - p_0\right)\times\left[1 - \exp\left(-\frac{2K\tan\delta}{L}H\right)\right]\right\} \quad (7b)$$

Equations 4 and 5 are used in the presence of a tension crack.

Li & Aubertin (2014) used FLAC3D to evaluate the response of cemented fill upon vertical exposure. Their results indicated that the shear resistance along sidewalls for the lower block acts parallel to the sliding surface. The sliding wedge (see Figure 1) is then divided into an upper rectangular block and a lower triangular wedge. The interface cohesion along the back wall was taken into account. These assumptions lead to the following expression for HAR stopes:

$$c=\frac{D'\left(p_0+\gamma\left(H-H'\right)-G'\right)+\frac{\gamma A'H'}{2}\left(1+\frac{L}{B}\right)\sin\alpha-\gamma\left(\frac{C'}{M}+\frac{H'}{2}\right)}{B'\left(1+\frac{L}{B}\right)+D'\left(H-H'\right)\left(\frac{2r_s}{L}+\frac{r_b}{B}\right)}\text{, for FS= 1} \tag{8a}$$

with

$$A'=FS-\frac{\tan\phi'}{\tan\alpha}\qquad B'=\frac{1}{\cos\alpha}+r_s\frac{H'}{L}\qquad C'=\frac{1-\exp\left(-MH'\right)}{MH'}-1\qquad D'=A'\left(1+\frac{L}{B}\right)\sin\alpha+C' \tag{8b}$$

$$H'=B\tan\alpha\qquad M=2K\left(B^{-1}+L^{-1}\right)\tan\delta\qquad G'=\frac{1}{1+L/B}\left\{\gamma\left(H-H'\right)+\left(p_0-\frac{\gamma}{M}\right)\left[1-\exp\left(-\left(H-H'\right)M\right)\right]\right\} \tag{8c}$$

These modified solutions were shown to be able to better represent the experimental data reported by Mitchell et al. (1982), than the original Mitchell solution. These solutions are assessed using numerical simulations in the following sections.

3 Numerical simulations with FLAC3D

3.1 Numerical model

Figure 2 illustrates the numerical model built with FLAC3D (Itasca Consulting Group, Inc. 2013) to investigate the mechanical behaviour of the exposed fill upon vertical exposure.

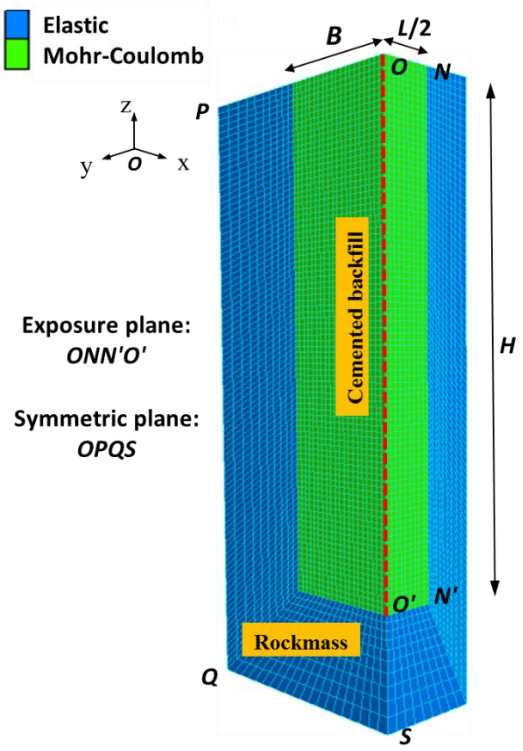

Figure 2 Numerical model of a side-exposed backfill in a primary stope built with FLAC3D

The rock mass is considered linearly elastic and characterised by a unit weight γ_r of 27 kN/m^3, a Young's modulus E_r of 30 GPa and a Poisson's ratio v_r of 0.3. The cemented backfill behaves as a Mohr–Coulomb elastoplastic material. The tensile strength cut-off T_0 is taken as nil, which corresponds to the most conservative case. The effective friction angle of fill ϕ' is related to its Poisson's ratio v through the relationship $v = (1 - \sin\phi')/(2 - \sin\phi')$, based on the uniqueness and consistency of at-rest earth pressure coefficient K_0 (Falaknaz 2014; Jahanbakhshzadeh 2016; Yang 2016). The stope geometry and fill properties for various simulated cases are summarised in Table 1.

Table 1 Stope geometry for various cases simulated using FLAC3D; other fill properties: $\phi' = 35°$ and related $v = 0.3$, $T_0 = 0$ MPa, dry unit weight $\gamma = 18$ kN/m^3, Young's modulus $E = 300$ MPa, and dilation angle $\psi = 0°$

Case	*H* (m)	*B* (m)	*L* (m)	Figure
1	45	6	9	3
2	45	10, 16, 25	9	4
3	Variable	6	9	6a
4	45	Variable	9	6b
5	45	6	Variable	6c

Displacements are prevented in all directions at outer boundaries of the rock mass (except for the top surface). On the symmetry plane $x = 0$, displacements are restricted in the x direction and allowed in the y and z directions (Figure 2). Meshing is based on the sensitivity analysis presented in Yang (2016). The primary stope is first excavated in one step and then filled with 5 m/layer. The exposure is created by instantly removing the constraint along the open face. This corresponds to the limit equilibrium method used in the theoretical development. A novel instability criterion (see Section 3.2) is applied to assess the failure of the exposed fill. The strength reduction analysis is performed to determine the minimum required fill cohesion. Interface elements are not used along the fill–wall contacts (e.g. Li & Aubertin 2009; Liu et al. 2016).

3.2 Failure mode and instability criterion

The failure of the exposed fill is commonly evaluated by the yield state, shear strength ratio, displacement and tensile stresses (Coulthard 1999; Pierce 2001; Falaknaz 2014; Li & Aubertin 2014; Liu et al. 2016). However, the stability evaluation based on these criteria can sometimes lead to ambiguous judgement. A new instability criterion is defined here based on the total displacement along the vertical centreline of the exposure (dotted line OO' in Figure 2). This method is inherited from the instability criterion used to assess the stability of a structure, instead of the failure or yield state of a material (Yang et al. 2017a).

Numerical results shown in Figure 3 illustrate the typical variation of the total displacement along the stope depth h (line OO' in Figure 2; Case 1 in Table 1). The maximum total displacement increases slightly (in mm) when the c value goes from 30 to 25 kPa, and surges dramatically to about 1 m for a continuous reduction of c to 24 kPa. Such dramatic increase of the displacement with slightly reduced backfill cohesion indicates the onset of failure of the exposed fill (see more details presented in Yang 2016).

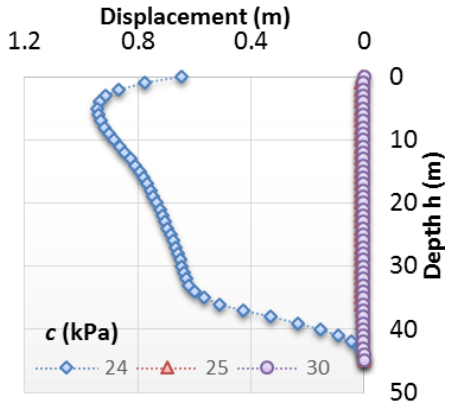

Figure 3 Displacement profiles along the stope depth *h* (line OO′ in Figure 2) for different values of backfill cohesion *c* (Case 1 in Table 1)

The failure mode assumed in existing analytical solutions considers a planar slip surface (see Figure 1). This is confirmed in the laboratory tests conducted by Mitchell et al. (1982). However, such failure mode only governs for relatively small backfill cohesion. New numerical results shown in Figure 4 indicate that the slip surface can become spoon-shaped when the stope geometry requires a larger cohesion (e.g. Falaknaz 2014). This is due to the build-up of tensile stresses near the fill top, which also renders the required *c* independent of stope width *B* (see Figure 4). Such failure mode has been confirmed by centrifuge tests performed on cemented fills (Mitchell 1986; Dirige & De Souza 2000, 2013) and field observations (e.g. Emad et al. 2014). A new analytical solution is thus required.

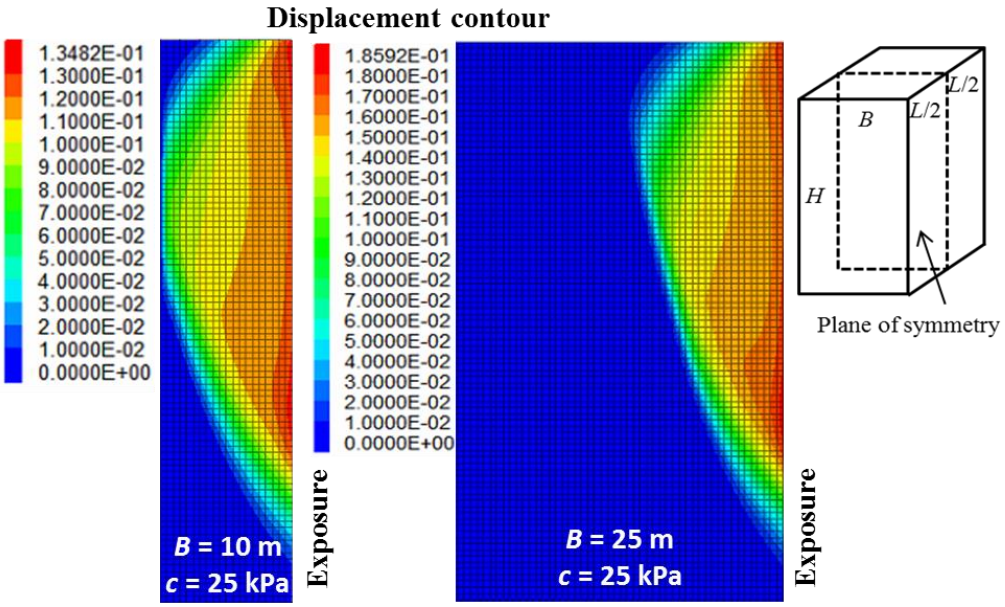

Figure 4 Displacement contours along the vertical plane of symmetry of the exposed fill at a critical state for different values of stope width *B* (from 10 to 25 m; Case 2 in Table 1)

4 Proposed solution and its validation

4.1 Modified formulation

Figure 5 shows the theoretical model consisting of a slip wedge and a tension crack. The weight of the wedge is denoted by W and the slip plane is inclined at an angle α of 45° + $\phi'/2$ to the horizontal. S_s is the shear forces acting along the sidewalls. S_t is the shear forces (due only to fill cohesion) along the (potential) tension crack; the frictional strength mobilised along this crack is neglected. H_t (m) is the depth of the tension crack and B_t (m) is the equivalent width of the wedge.

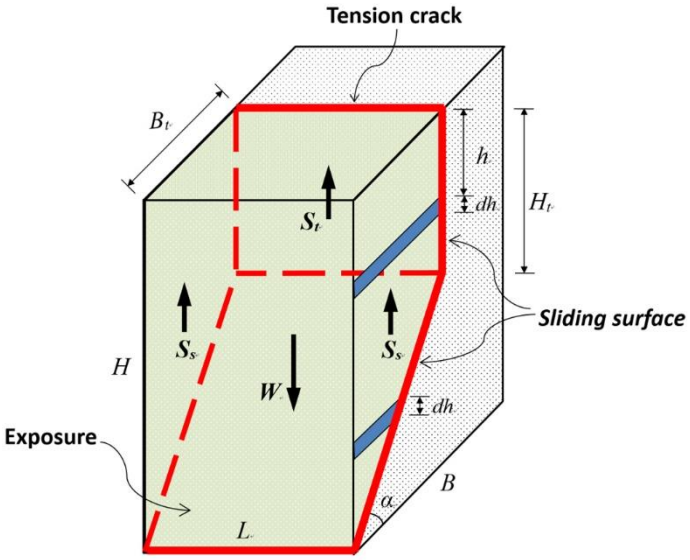

Figure 5 Modified wedge model with a vertical tension crack (adapted from Li & Aubertin 2012)

Based on the Mohr–Coulomb criterion, the shear strength available at the fill–sidewall interface τ_s is given by:

$$\tau_s = c_s + \sigma_h \tan\delta \tag{9}$$

where:

c_s ($= r_s c$, $0 \le r_s \le 1$) is the interface cohesion along the sidewalls.

σ_h is the horizontal stress along the sidewalls at depth h (Figure 5).

The value of σ_h is obtained with the following expression (Li et al. 2003):

$$\sigma_h = \frac{\gamma L}{2\tan\delta}\left[1 - \exp\left(-2K\tan\delta\frac{h}{L}\right)\right] \tag{10}$$

where:

K is taken as Rankine's active pressure coefficient $K_a = (1-\sin\phi')/(1+\sin\phi')$.

The shear force acting along a fill–sidewall interface S_s is expressed as (see Figure 5):

$$S_s = \int_0^{H_t} \tau_s B_t dh + \int_{H_t}^{H} \tau_s \frac{H-h}{\tan\alpha} dh \tag{11}$$

where:

B_t is estimated from Equation 5.

Introducing Equations 9 and 10 into Equation 11, the expression of S_s is written as:

$$S_s = B_t\left(r_s c + \frac{\gamma L}{2}\right)\left(H - \frac{B_t\tan\alpha}{2}\right) - \frac{\gamma B_t L^2}{4K\tan\delta} + \frac{\gamma L^3}{8K^2\tan\alpha\tan^2\delta}\left[\exp\left(-\frac{2K\tan\delta}{L}H_t\right) - \exp\left(-\frac{2K\tan\delta}{L}H\right)\right] \tag{12}$$

The net weight of the slip wedge W_n is given by:

$$W_n = W - 2S_s - S_t \tag{13}$$

where:

The self-weight of the wedge $W = \gamma B_t L[H - (B_t\tan\alpha)/2]$.

The shear force acting along the tension crack $S_t = cH_tL$; H_t is obtained with Equation 4.

The FS of the sliding wedge is written as:

$$FS = \frac{W_n \cos\alpha \tan\phi' + cLB_t / \cos\alpha}{W_n \sin\alpha} = \frac{\tan\phi'}{\tan\alpha} + \frac{2}{\sin 2\alpha}\frac{cLB_t}{W_n} \tag{14}$$

Introducing Equations 12 and 13 into Equation 14, the limit equilibrium analysis of the slip wedge leads to the proposed solution in terms of the required fill cohesion c:

$$c = p\left[\frac{2}{(FS - \tan\phi'/\tan\alpha)\sin 2\alpha} + \frac{H_t}{B_t} + r_s\frac{2H - B_t\tan\alpha}{L}\right]^{-1} \tag{15a}$$

with

$$p = \frac{L}{2K\tan\delta}\left\{\gamma - \frac{\gamma L}{2KB_t\tan\delta\tan\alpha}\left[\exp\left(-\frac{2K\tan\delta}{L}H_t\right) - \exp\left(-\frac{2K\tan\delta}{L}H\right)\right]\right\} \tag{15b}$$

where:

B_t is estimated from Equation 5, and p (Equation 15b) is used to simplify Equation 15a.

4.2 Validation using numerical simulations

The proposed analytical solution is compared to the numerical simulations, as illustrated in Figure 6, in terms of the required (critical) fill cohesion c against stope geometry (Cases 3, 4 and 5 in Table 1). The critical fill cohesions obtained by numerical simulations are determined using the instability criterion based on displacement. Four existing analytical solutions (Mitchell et al. 1982; Li & Aubertin 2012, 2014; Li 2014) are also shown for comparison. The required c value obtained with numerical simulations increases with an increase in stope length L (Figure 6(a)) and (to a lesser extent) in stope height H (Figure 6(b)). The numerical results are almost independent of the stope width B (Figure 6(b)).

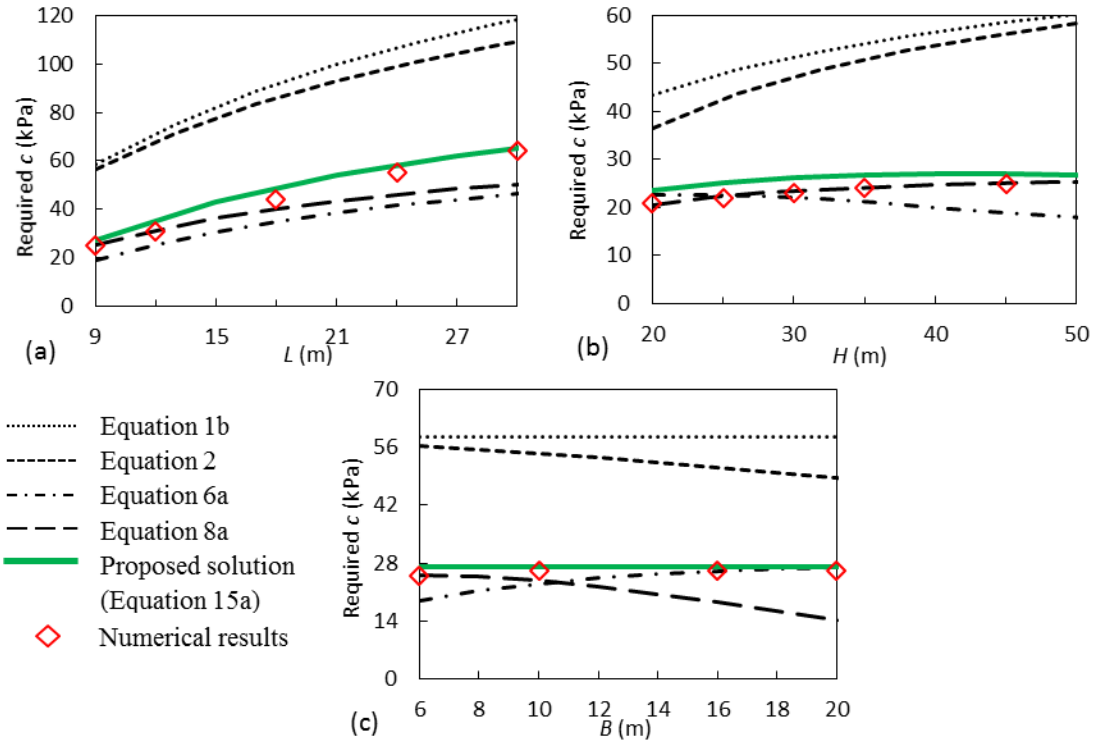

Figure 6 **Required backfill cohesion c estimated from Equation 15a and four other analytical solutions, and numerical simulations, for different values of stope (a) height H (Case 3 in Table 1), (b) width B (Case 4 in Table 1), and (c) length L (Case 5 in Table 1). Calculations made with Equation 15a for FS = 1, $\phi' = \delta = 35°$, $r_s = 1$, $\gamma = 18$ kN/m^3**

The results indicate that improvements are obtained by the modified analytical solutions, while Equations 1b and 2 largely over-predict the required fill cohesion (relative to other numerical and analytical approaches). Figure 6(a) and 6(c) indicate that the proposed solution (Equation 15a) agrees with the simulation results. When stope height H increases, the required c values obtained with Equation 15a slightly increase for $H \leq 45$ m and then slightly decline for $H > 45$ m. Nonetheless, the proposed solution agrees fairly well with simulation results for an exposed height from 20 to 50 m.

Additional results indicate that both the analytical and numerical solutions predict a reduction in the required cohesion (and agree well with each other) as the ϕ' value increases (from 1 to 45° with the related v value varying from 0.496 to 0.227; see more details in Yang (2016) and Yang et al. (2017b)).

These results indicate that the proposed analytical solution (Equation 15a) correlates well with the numerical simulations for typical stope sizes and fill properties. However, the numerical and analytical results are based on the consideration that the fill–wall interfaces have the same mechanical properties as the backfill. Several laboratory tests have shown that this is not fully representative (Fall & Nasir 2010; Koupouli et al. 2016). More work is needed to take into account interfaces between the backfill and walls.

5 Conclusions

Numerical simulations are performed with FLAC3D using the elasto-plastic model, considering related effective friction angle ϕ' and Poisson's ratio v of the backfill. An instability criterion is defined to assess more objectively the stability of backfill upon exposure from numerical simulations. These results show that the required cohesion of the cemented fill mainly depends on the backfill exposure length L, and almost insensitive to the stope width B, due to the build-up of tensile stresses near the backfill top surface. A new analytical solution is proposed to evaluate the stability of exposed cemented backfill, using a combination of an inclined and a vertical planar surface. The results indicate that the proposed solution agrees well with the numerical simulations for typical stope geometries and fill properties.

Acknowledgement

The authors acknowledge the financial support from the Natural Sciences and Engineering Research Council of Canada (NSERC), Institut de recherche Robert-Sauvé en santé et en sécurité du travail (IRSST), Fonds de recherche du Québec - Nature et Technologies (FRQNT) and the industrial partners of the Research Institute on Mines and Environment (RIME UQAT-Polytechnique; http://rime-irme.ca/en).

References

Askew, J, McCarthy, PL & Fitzgerald, DJ 1978, 'Backfill research for pillar extraction at ZC/NBHC', *Proceedings of 12th Canadian Rock Mechanics Symposium on Mining with Backfill*, Canadian Institute of Mining, Metallurgy and Petroleum, Westmount, pp. 100–110.

Bowles, JE 1984, *Physical and Geotechnical Properties of Soils*, 2nd edn, McGraw–Hill, New York.

Coulthard, MA 1999, 'Applications of numerical modelling in underground mining and construction', *Geotechnical and Geological Engineering*, vol. 17, no. 3–4, pp. 373–385.

Dirige, APE & De Souza, E 2000, 'Centrifuge physical modelling of paste fill designs for improved cost performance', *Proceedings of the Millennium 2000 CIM Conference*, Canadian Institute of Mining, Metallurgy and Petroleum, Westmount.

Dirige, APE & De Souza, E 2013, 'Mechanics of failure of paste backfill face exposure during adjacent mining', *Proceedings of 23rd World Mining Congress*, Canadian Institute of Mining, Metallurgy and Petroleum, Westmount.

Dirige, APE, McNearny, RL & Thompson, DS 2009, 'The effect of stope inclination and wall rock roughness on back–fill free face stability', in M Diederichs & G Grasselli (eds), *Proceedings of the 3rd Canada–US Rock Mechanics Symposium: Rock Engineering in Difficult Conditions,* (CD–ROM), Omnipress, Madison.

Emad, MZ, Mitri, H & Kelly, C 2014, 'Effect of blast–induced vibrations on fill failure in vertical block mining with delayed backfill', *Canadian Geotechnical Journal*, vol. 51, no. 9, pp. 975–983.

Falaknaz, N 2014, 'Analysis of geomechanical behavior of two adjacent backfilled stopes based on two and three dimensional numerical simulations', PhD thesis, Mineral Engineering, Polytechnique Montreal, Montreal.

Falaknaz, N, Aubertin, M & Li, L 2015, 'On the stability of exposed backfill in mine stopes', *Proceedings of the 68th Canadian Geotechnical Conference*, Canadian Geotechnical Society, Quebec.

Fall, M & Nasir, O 2010, 'Mechanical behaviour of the interface between cemented tailings backfill and retaining structures under shear loads', *Geotechnical and Geological Engineering*, vol. 28, no. 6, pp. 779–790.

Itasca Consulting Group, Inc., 2013, *FLAC3D: Fast Lagrangian Analysis of Continua in 3 Dimensions; User's Guide*, Itasca Consulting Group, Inc., Minneapolis.

Jahanbakhshzadeh, A 2016, *Analyse du Comportement Géomécanique des Remblais Miniers dans des Excavations Souterraines Inclines*, PhD thesis, Mineral Engineering, Polytechnique Montreal, Montreal.

Koupouli, NJ, Belem, T, Rivard, P & Effenguet, H 2016, 'Direct shear tests on cemented paste backfill–rock wall and cemented paste backfill–backfill interfaces', *Journal of Rock Mechanics and Geotechnical Engineering*, vol. 8, pp. 472–479.

Li, L 2014, 'Generalized solution for mining backfill design', *International Journal of Geomechanics*, vol. 14, no. 3, pp. 04014006.

Li, L & Aubertin, M 2009, 'Numerical investigation of the stress state in inclined backfilled stopes', *International Journal of Geomechanics*, vol. 9, no. 2, pp. 52–62.

Li, L & Aubertin, M 2012, 'A modified solution to assess the required strength of exposed backfill in mine stopes', *Canadian Geotechnical Journal*, vol. 49, no. 8, pp. 994–1002.

Li, L & Aubertin, M 2014, 'An improved method to assess the required strength of cemented backfill in underground stopes with an open face', *International Journal of Mining Science and Technology*, vol. 24, no. 4, pp. 549–558.

Li, L, Aubertin, M, Simon, R, Bussière, B & Belem, T 2003, 'Modelling arching effects in narrow backfilled stopes with FLAC', *Proceedings of* the *3rd International Symposium on FLAC & FLAC 3D Numerical Modelling in Geomechnics*, CRC Press, Boca Raton, pp. 211–219.

Liu, G, Li, L, Yang, X & Guo, L 2016, 'Numerical modelling of the stability of cemented backfill with a vertical face exposed: a revisit to Mitchell's physical model tests', *International Journal of Mining Science and Technology*, vol. 26, no. 6, pp. 1135–1144.

McCarthy, DF 2002, *Essentials of Soil Mechanics and Foundations: Basic Geotechnics*, 6th edn, Prentice Hall, Englewood Cliffs.

Mitchell, RJ 1986, 'Centrifuge model tests on backfill stability', *Canadian Geotechnical Journal*, vol. 23, no. 3, pp. 341–345.

Mitchell, RJ, Olsen, RS & Smith, JD 1982, 'Model studies on cemented tailings used in mine backfill', *Canadian Geotechnical Journal*, vol. 19, no. 1, pp. 14–28.

Pierce, ME 2001, 'Stability analysis of paste back fill exposes at Brunswick Mine', *Proceedings of the 2nd International FLAC Symposium,* Swets & Zeitlinger Publishers, Lisse, pp. 147–156.

Yang, PY 2016, *Investigation of the Geomechanical Behavior of Mine Backfill and its Interaction with Rock Walls and Barricades*, PhD thesis, Mineral Engineering, Polytechnique Montreal, Montreal.

Yang, PY, Li, L & Aubertin, M 2017b, 'A new solution to assess the required strength of mine backfill with a vertical exposure', *International Journal of Geomechanics*, vol. 17, no. 10.

Yang, PY, Li, L, Aubertin, M, Brochu–Baekelmans, M & Ouellet, S 2017a, 'Stability analyses of waste rock barricades designed to retain paste backfill', *International Journal of Geomechanics*, vol. 17, no. 3, pp. 04016079.

Zou, DH & Nadarajah, N 2006, 'Optimizing backfill design for ground support and cost saving', *Proceedings of the 41st US Rock Mechanics Symposium: 50 Years of Rock Mechanics*, American Rock Mechanics Association, Alexandria.